Behavior Research Methods, Instruments, & Computers
1984, 16 (4), 341-350

METHODS & DESIGNS

Instrument considerations in measuring fast eye movements

CHRISTOPHER M. HARRIS, ISRAEL ABRAMOV, and LOUISE HAINLINE
Brooklyn College, City University of New York, Brooklyn, New York

The dynamic limitations of eye movement recorders can distort the measurement of fast eye movements such as saccades and nystagmic quick phases. In this paper, the effects of the bandwidth and noise of recording methods and the problems incurred by digital sampling are discussed theoretically with respect to the measurement of peak velocity and duration of fast eye movements. As a practical example, a TV-based infrared corneal reflex system is examined and a method for calibrating it for peak velocity measurement is described.

The measurement of eye movements (EMs) is becoming increasingly relevant in fields other than those concerned with the analysis of the oculomotor system itself. For example, correlations between unusual EMs and neurological pathologies have been made by Hamann (1979) and Zee, Optican, Cook, Robinson, and Engel (1976). There is also a large body of literature on the relationship between reading and EMs (e.g., Levy-Schoen & O'Regan, 1979). Furthermore, EM measurement is beginning to be used in the developmental study of the human infant (Aslin & Salapatek, 1975; Hainline, 1981). Each application of EM measurements has its own technological priorities. Some research questions require that the measuring system have great speed and resolution, whereas others require that intrusiveness upon the subject be minimized. In most current systems, there is a tradeoff among resolution, intrusiveness, and, of course, cost.

The various instruments and their merits have been discussed elsewhere (e.g., see Young & Sheena, 1975, for a comprehensive review). However, for efficient progress, it is essential to be able to compare data from different instruments in different settings. To this end, McConkie (1981) stressed the need for investigators to report the quality of their data, such as sampling rate, drift, noise, accuracy, and short- and long-term repeatability. But such reporting necessitates an intimate understanding of one's EM recording instrument.

The need for calibrating an instrument so that the direction of the subject's eye is precisely mapped onto stimulus space is self-evident, and there are various schemes for doing this (Bullinger & Kaufmann, 1977); Carmody, Kundel, & Nodine, 1980; Harris, Hainline, & Abramov, 1981; Kliegl & Olson, 1981; Mendelson, Haith, & Goldman-Rakic, 1981). It is less appreciated, though, that even an accurate mapping procedure does not calibrate the instrument for all purposes. For example, during measurement of fast EMs such as saccades or nystagmic quick phases, the bandwidth and noise of the recording system can degrade the recording of dynamic responses. The most commonly used parameters for describing fast EMs are peak velocity (PV) and duration. In this paper, we discuss the general effects of a system's bandwidth and noise on the measurement of these two parameters of fast EMs. As an example, we present the results of a dynamic calibration of a TV-based, infrared, corneal-reflex system (Hainline, 1981) for the measurement of PV. Although this kind of instrument is certainly less than ideal for recording fast EMs, it has the advantage of being nonintrusive to the subject, which makes it useful for recording from infants and young children. We show that PVs of fast EMs can be recovered from such slow eye trackers, thereby increasing the information that can be derived from their recordings. Even though a slow system is used as an example, the arguments we present are generally applicable to all eye trackers.

This work was supported in part by Grants 13484 and 662199 from the PSC-CUNY Research Award Program and NIH Grant EY-03957.
The authors' mailing address is: Department of Psychology, Brooklyn College of CUNY, Brooklyn, NY 11210.

THEORETICAL CONSIDERATIONS

Bandwidth

The first consideration is the effect of the recording instrument's bandwidth on the integrity of fast EM data. Here, the recording instrument is taken to include all aspects of the system (except the subject) and also any digitization process for on- or off-line computation. The final recording of the EM will be called the output of the instrument, o(t). During a fast EM such as a saccade, the eye position, e(t), changes rapidly in time with some profile. This profile can be broken down into its spectrum of frequencies, E(f), by Fourier analysis, with the result that, the faster the EM, for a given amplitude, the more pronounced are its higher frequency components. If the

instrument acts as a low-pass filter, these higher frequency components will be attenuated and an apparently slower movement will be recorded. Consequently, the duration of the EM would be overestimated. Equivalently, bandwidth distortion results from an instrument with a time constant comparable to, or longer than, the EM itself.

The relationship between the output and the EM is illustrated in stylized form in Figure 1, and can be summarized by:

$$O(f) = H(f)E(f). \quad (1)$$

We will follow the convention that functions denoted by uppercase refer to the Fourier transform of the corresponding temporal functions in lowercase.[1] Here, E(f) is the Fourier transform of the EM, e(t); H(f) is the transfer function of the instrument or the profile of its filtering action; and O(f) is the transform of the output, o(t). The actual time course of the output can be recovered from Equation 1 by taking inverse Fourier transforms (e.g., Champeney, 1973):

$$o(t) = \int_{-\infty}^{\infty} h(\tau)e(t-\tau)d\tau. \quad (2)$$

The output will be a faithful representation of the EM only if the instrument's filtering profile is flat to at least the highest frequency component in the EM. Although EMs do not have a cutoff frequency, but approach zero asymptotically, from a practical point of view they have effective components up to about 50 Hz (see Zuber, Semmlow, & Stark, 1968).

It is frequently more relevant to consider eye velocity rather than eye position, and to find the relationship between the instrument's output velocity, v(t), and the actual eye velocity, $\dot{e}(t)$ (the time derivative of a function will be denoted by a dot over it). This can be found by taking the time derivative of Equation 2 (see also Figure 1):

$$v(t) = \int_{-\infty}^{\infty} h(\tau)\dot{e}(t-\tau)d\tau. \quad (3)$$

Equations 2 and 3 are similar because the instrument has been considered to be linear and time-independent. Although the filtering action of the instrument on its input has not changed, it now acts on eye velocity rather than position. By taking the Fourier transform of Equation 3, the spectrum of the output velocity, V(f), is given by:

$$V(f) = H(f)\dot{E}(f) = 2\pi jfH(f)E(f). \quad (4)$$

The spectrum of the actual eye velocity, $\dot{E}(f)$, differs from the eye position spectrum by the factor $2\pi jf$. Apart from a phase lead of 90°, this factor indicates that the magnitude of any frequency component in the position spectrum must be multiplied by the frequency of that component to give the corresponding magnitude of the component in the velocity spectrum. In other words, the higher frequency components of the velocity profile are more prominent than those of the position profile, so that any filtering distortion will be worse for velocity measurements than for position measurements. Therefore, it is important to bear in mind that velocity recording requires a higher bandwidth for a given accuracy.

In order to quantify the effect of suboptimal bandwidth, it is necessary to specify shapes for the EM profile, e(t) or E(f), and the filtering action of the instrument, H(f). For clarity, we will represent a fast EM by a unit step function. Although this is an extreme case, its mathematical treatment is simple; later we will introduce a more realistic representation. A step input has infinite velocity and infinitessimal duration and thus represents a physically limiting case. The velocity profile of this idealized input is given by the impulse function, which has a spectrum of unity. Thus, from the inverse transform of Equation 4, the velocity profile of the output will be:

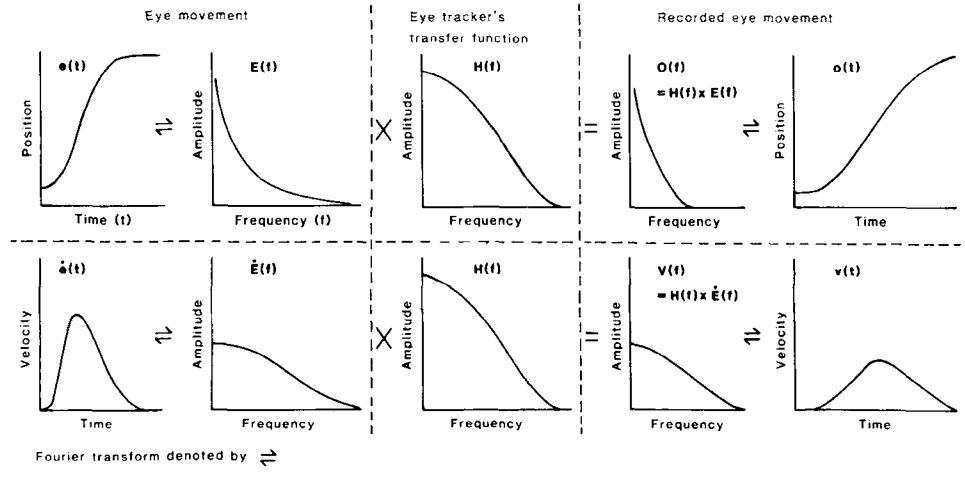

Figure 1. Stylization of the possible effect of an eye movement recorder on a saccade. Top row shows the transfer of the positional signal of the eye movement. Bottom row shows the transfer of the velocity signal. Note the reduction in peak velocity and the increase in duration caused by using an instrument with too-limited bandwidth.

$$v(t) = \int_{-\infty}^{\infty} H(f)e^{2\pi jft}df. \quad (5)$$

This result is quite general for any physically realizable system. In any system, there will be a delay between input and output; however, provided this delay is the same for all input frequency components, the system acts as a pure-delay passive filter. As a consequence, the pure delay can be ignored, but not forgotten, and the output velocity of such a filtering system is given simply by the real part of Equation 5:

$$v(t) = 2\int_{0}^{\infty} H(f)\cos(2\pi ft)df. \quad (6)$$

This output has two important features. First, the peak velocity (PV) will always occur at t = 0 (since pure delay is being ignored and the input is a step function), and will be given by:

$$PV = 2\int_{0}^{\infty} H(f)df. \quad (7)$$

In other words, the maximum velocity that such an instrument can yield for a unit step input is equal to twice the area under the instrument's filtering profile (including positive frequencies only). For example, consider the instrument's filtering profile to be that of a low-pass rectangular filter with a cutoff frequency of 20 Hz. For a 1° step input, the peak output velocity will be reduced to 40°/sec by the bandwidth of the instrument. Similarly, for a 10° step input, the peak output velocity will be 400°/sec.

The second feature of Equation 6 is that it permits the calculation of duration of the output provided H(f) is known. If the start and end of the output are defined as occurring when velocity just reaches zero, from a rectangular filter with a cutoff frequency f_0, the duration of the output will be given by $1/f_0$ for a step input of *any* amplitude. Thus, any step input to a 20-Hz low-pass rectangular filter will yield an output with a duration of 50 msec. Of course, the durations of real EMs will vary with amplitude, but it will not be possible to record accurately durations less than the minimum duration imposed by the instrument's bandwidth.

These examples illustrate the effect of bandwidth in the limiting case. Actual fast EMs are not step functions, but have finite PVs and nonzero durations. In order to be more realistic, it is useful to model the human saccadic system so that computations can easily be made. It is well established from physiological work that the saccade is generated by the action of a combination of a phasic pulse and a tonic step input to the extraocular muscles (e.g., Robinson, 1981). We therefore idealize the saccadic generator as a second-order system with both accelerative and velocity terms. Actual values for the time constants of these terms are taken from Zee and Robinson (1979). The driving input for this system is idealized as a rectangular pulse superimposed on a step. No assumption is made concerning the mechanism involved in determining the pulse width and pulse height relative to the step height. Values for these parameters are taken from Collins (1974) and are slightly modified, when necessary, to generate saccades with typical PVs and durations. These approximations provide a means of generating a reasonable facsimile of a human adult saccade in the computer, from which spectra and the effects of bandwidth can be computed. We have chosen to simulate fast EMs according to the above model for the sake of computational simplicity. The general conclusions are affected only in detail by variations in the EM profile. Figure 2 shows the effect of a recording system with a rectangular filtering profile on these simulated saccades. The solid lines represent responses to simulated saccades, and the dashed lines depict responses to ideal step inputs; amplitudes range from 5 to 30°. In Figure 2a, each curve plots the PVs and durations that would be measured for any one EM by a system with a low-pass rectangular filtering profile with a cutoff frequency, f_0, shown along the abcissa. For ex-

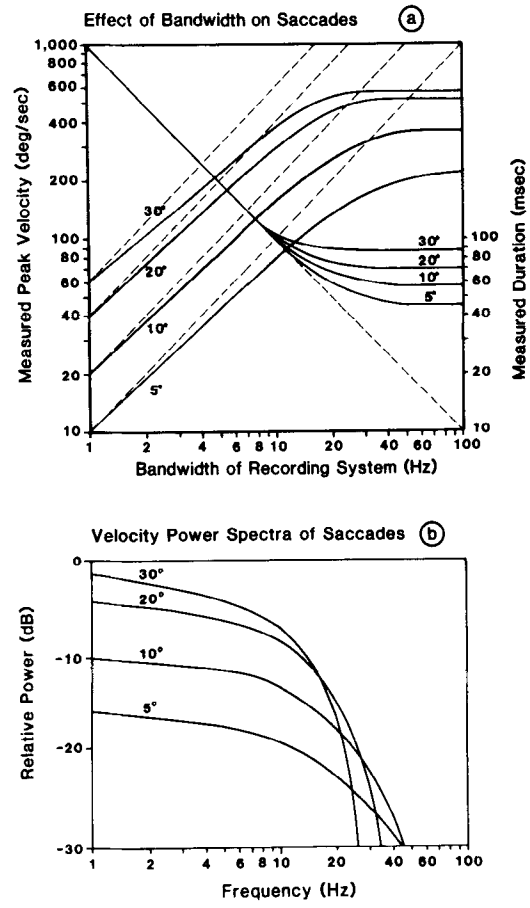

Figure 2. Effect of eye movement recording instrument's bandwidth on computer-simulated saccades (solid lines) and step inputs (dashed lines). (a) The left-hand ordinate shows the peak velocity that would be measured for 5-, 10-, 20-, and 30° simulated saccades and step inputs by an instrument with a rectangular low-pass filtering profile with a cutoff frequency shown along the abscissa. The right-hand ordinate shows the measured duration of the instrument's output for the same inputs. (b) Power spectra of the velocity of the simulated saccades in decibels, normalized to a 30° saccade.

ample, consider a simulated 10° saccade. If the cutoff frequency of the instrument is 10 Hz, the measured PV will be only about 150°/sec, as opposed to an actual PV of about 350°/sec (see asymptote of 10° curve); to measure this true PV, an instrument cutoff frequency of at least 50 Hz is needed. For the same 10° simulated saccade with an instrument cutoff frequency of 10 Hz, measured duration will be 100 msec, instead of about 55 msec. Figure 2b shows the power spectra, measured in decibels, for the velocity of the simulated saccades and step inputs; the spectra have been normalized with respect to a 30° saccade.

As expected from the above discussion, once the bandwidth of the instrument's filtering profile exceeds that of the saccade, the measured PV and duration will be accurate. For instrument bandwidth below about 50 Hz, however, distortion becomes pronounced, giving rise to an underestimation of PV and an overestimation of duration. These effects are particularly important for shorter saccades, whose power spectra contain higher frequency components. The change in spectra with amplitude is a direct consequence of the step-pulse mechanism that generates saccades; the pulse is more prominent for shorter saccades, but the step is dominant in larger saccades. For very low instrument bandwidths, the output is determined almost entirely by the instrument's bandwidth, and no information about the input profile (except amplitude) can be recorded. Another consequence of low bandwidth (not shown here) is "ringing." This easily can be mistaken for, or can obscure, actual overshoots in EMs.

Noise

Our second major consideration is the effect of noise on the measurement of fast EMs. Only noise with sufficient bandwidth to distort the profile of a fast EM will be considered here; slow "dc" drifts, commonly found in electrooculograms (EOGs), will be ignored because they belong more to the realm of static calibration. Four independent noise sources are identified.

(1) Holder. Noise may originate in the device, or the person, holding the subject's head stationary. Vibrations transmitted to the subject via a chinrest or bitebar are small in the laboratory environment. Detectable head movements are more likely to occur if the subject's head is minimally restrained (e.g., Bronson, 1982; Haith, 1980) or is held by an assistant (Hainline, 1981), which is the case with infant subjects.

(2) Head movements. This source of noise is distinguished from the above in that it originates in the subject rather than in the environment. At one extreme, the dental bitebar represents the most effective (and intrusive) means of eliminating head movements for human subjects. At the other extreme, the head is allowed to move freely within a restricted region, and head movements are corrected electronically or optically. This compensation must require the detection of head movements, and it will not only leave a residual noise, but also have a finite bandwidth, thereby increasing the possibility of error caused by fast head movements. Since, in free viewing, saccades often precede head movements, a strong possibility of signal-dependent noise arises.

(3) Oculomotor noise. Oculomotor noise may be considered as time variations in extraocular muscle tension, neuronal shot noise, any noise in the target localization process of the subject, and so forth. Unlike the other noise sources, this noise cannot be considered to be an artifact, since it is inherent in the system under scrutiny.

(4) Recording system noise. As with any other measuring device, the instrument will introduce its own noise. The most sensitive part of most instruments in this respect is the detector, namely, the receiving coil, electrodes, photomultiplier, photodiode(s), or TV camera. Although most system noise will originate at this level, significant sources, such as amplifier noise and analog-to-digital conversion noise, may be injected later in the system.

Usually, noise from these sources will combine independently and will be filtered by the instrument along with the actual eye position signal. The noise at the output will therefore also be band limited. If the combined noise referred to the instrument's input has a power spectrum given by N(f), then, for measures of eye position, the root-mean-square (RMS) noise appearing at the output will be given by (see, e.g., Pierce & Posner, 1980):

$$\sigma_{pos} = \left[\int_{-\infty}^{\infty} N(f)|H(f)|^2 df\right]^{1/2}. \quad (8)$$

This describes the well-known phenomenon that, the greater the bandwidth of a recording system, the greater the RMS noise will be at the output. For the sake of illustration, consider the instrument filtering profile to be a low-pass rectangle with cutoff f_0, and also assume the noise to be white and gaussian with a spectral power density of $N_0/2$. For this case, the RMS positional noise will be given by $(N_0 f_0)^{1/2}$. In other words, the standard deviation of the noise appearing on the position data will be proportional to the square root of the bandwidth of the instrument.

Since velocity measures contain augmented high-frequency components (see Equation 4), velocity noise will be greater than position noise. The RMS noise on the velocity signal at the instrument's output will be given by:

$$\sigma_{vel} = 2\pi\left[\int_{-\infty}^{\infty} f^2 N(f)|H(f)|^2 df\right]^{1/2}. \quad (9)$$

If, as before, we assume a low-pass rectangular filter for H(f) and white noise, the standard deviation of the noise on the velocity signal will now be $2\pi(N_0 f_0^3/3)^{1/2}$; velocity noise now depends on bandwidth raised to 3/2, rather than 1/2. In short, extending the bandwidth of the instrument beyond that of the EM increases the noise unnecessarily.

The presence of velocity noise precludes the use of zero velocity as the criterion for deciding when a fast EM starts and stops, that is, its duration. It is therefore common to require that velocity fall below some small criterion.

However, this would underestimate the duration. Furthermore, if the criterion is held constant, this underestimation will be more severe for small saccades than for large saccades. Although this effect is small, it may confound the duration/amplitude relationship found for low-amplitude saccades ($<10°$) in human adults (e.g., Howard, 1982, p. 262). An alternative scheme is to allow the criterion to vary proportionately with the amplitude. This is particularly useful for noisy data, but becomes inoperative for small-amplitude movements, since the criterion will eventually become embedded in noise.

Sampling

Digitization of analog data for computer analysis must involve sampling. Analog-to-digital conversion may take place at such a fast rate that there is virtually no distortion in the measurement of PV or duration from digital records. However, systems that operate with TV video cameras have an intrinsic sampling problem, since eye position can be estimated no faster than TV field rate. In order to discuss sampling distortion, it is necessary to describe the sampling function utilized by the system. A signal can be sampled instantaneously every sampling period, or a sample can be obtained by averaging the signal throughout each sampling period. These sampling functions represent two extreme forms of sampling, and each has its own drawback. The instantaneous sampling function can give rise to serious aliasing problems. Aliasing occurs whenever there exist components in the input signal above half the sampling rate—the Nyquist, or "folding," frequency. The frequency of these components will be translated, or "folded back," to new frequencies below half the sampling rate, and will confound signal components already at these lower frequencies. For example, when sampling occurs at 60 Hz (TV rate), the Nyquist frequency is 30 Hz. If the input signal has a component at 50 Hz, it will appear in the sampled signal, not at 50 Hz, but at 10 Hz and will be superimposed on any original 10-Hz signal component. The usual remedy for aliasing is to filter out the signal components above the Nyquist frequency with a low-pass antialiasing filter before sampling takes place; however, this is free of distortion only if the sampling rate is at least twice the highest frequency component in the signal that is to be sampled. For fast EMs with a bandwidth of about 50 Hz (see Figure 2b), a minimum sampling rate of 100 Hz is needed. At the other extreme, a sampling function that lasts the whole sampling period reduces aliasing to a minimum, but at the expense of bandwidth. For this type of sampling function, any movement of the eye occurring within the sampling period will be lost or "smeared out," thus effectively reducing bandwidth. Formally, the filtering effect of sampling is given by the Fourier transform of the sampling function, so that the rectangular sampling function, lasting the whole sampling period, represents the worst case in lowering bandwidth. The filtering effects of sampling at 60 Hz for these two extremes are shown in Figure 3 (Curves a and b). Depending on the precise method of estimating eye position, TV systems will fall somewhere between these two extremes.

Another sampling problem, besides general bandwidth reduction and aliasing, is that of sampling error. It is common practice to estimate eye velocity by taking the difference between two samples of eye position and dividing

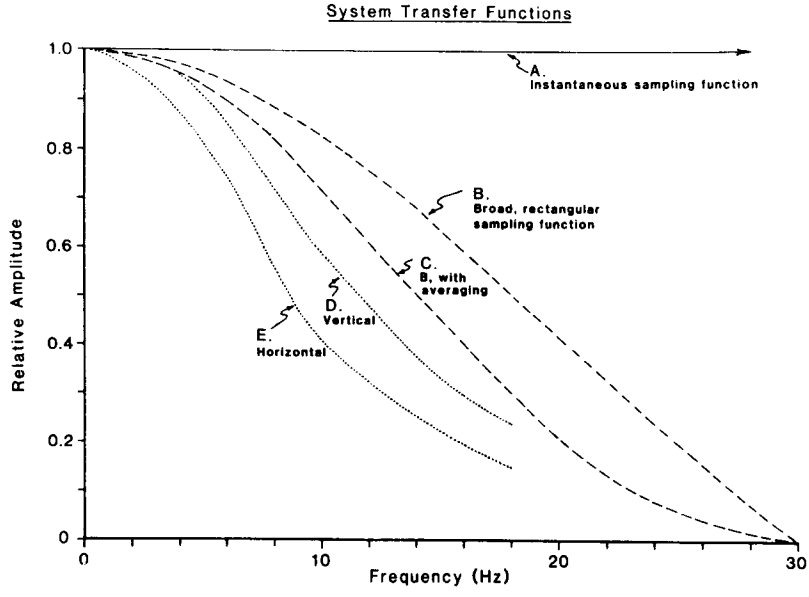

Figure 3. System transfer functions. (a) Due to an instantaneous sample taken at the sampling rate, r = 60 Hz. (b) Due to a rectangular sampling function lasting a complete sampling period: $\sin(2\pi f/r)/(2\pi f/r)$, r = 60 Hz. (c) Averaging consecutive samples obtained via (b). (d) Transfer function of the authors' instrument based on sinusoidally oscillating a mechanical "artificial eye" (see text) in the vertical plane. (e) Same as (d), but in the horizontal plane.

this by the interval. An estimate of eye velocity that is based on only two eye position samples is intrinsically inaccurate. This is true even if the sampling rate (r) is more than twice the signal bandwidth because, although the samples may contain all the information in the original eye position signal, the latter should first be reconstructed from the samples by filtering at the Nyquist frequency before differentiating to find velocity. If this is not done, the best estimate of eye velocity, $\hat{v}(t)$, based on two consecutive samples is given by:

$$\hat{v}(t) = \int_{-\infty}^{\infty} \dot{E}(f)H(f)\sin(\pi f/r)/(\pi f/r)e^{2\pi jft}df. \quad (10)$$

The sampling error term, $\sin(\pi f/r)/(\pi f/r)$, acts on the true velocity spectrum, $\dot{E}(f)$, in addition to the filtering profile of the instrument, H(f), which is in itself partly determined by the sampling function as described earlier. Thus, even if the sampling rate is more than the highest frequency component in the instrument's output, eye velocity will still always be underestimated when it is based on only two samples of eye position. An important case arises when PV is to be measured. If the true PV happens to occur in the middle of a sampling interval, then the underestimation will be at a minimum and is given by the above equation. If, however, the PV occurs elsewhere in the sample period, there will be further underestimation, the worst case arising when PV occurs at either end of a sampling period. To illustrate the degree of underestimation, consider the example shown in Figure 4a. For computational simplicity, a saccade is approximated by a step function passed through a low-pass rectangular filter with cutoff f_0 (the results of the computation would not be seriously changed if a more realistic EM were used). The bandwidth of the recording instrument can represent this filter. Without sampling, the measured PV would be equal to $2f_0$. However, when the output of the instrument's profile is sampled at k times f_0 (abcissa in Figure 4a), the percentage reduction in measured PV, for both best and worst cases, is shown along the ordinate. For example, in order to keep sampling error below 5%, a sampling rate of at least six times the instrument's bandwidth must be employed. Moreover, the absolute error will be proportional to PV, so that larger fast EMs with higher PVs will be prone to larger errors.

Another consequence of estimating eye velocity from only two samples is quantization error. Recording systems with high sampling rates are particularly prone to this error, which arises from the digitization process. It is best illustrated by example. Consider a system with 12-bit accuracy covering a full scale of 100° of eye movement. Each level of the output will correspond to 0.024°. If the sampling rate is 1 kHz, the minimum detectable velocity based on two consecutive samples would be 0.024° in 1 msec, or about 24°/sec. Thus, eye velocity could only be measured in steps of 24°/sec. On the other hand, a slower system with a 100-Hz sampling rate would measure eye velocity in steps of 2.4°/sec.

Sampling error, but not quantization error, can be made

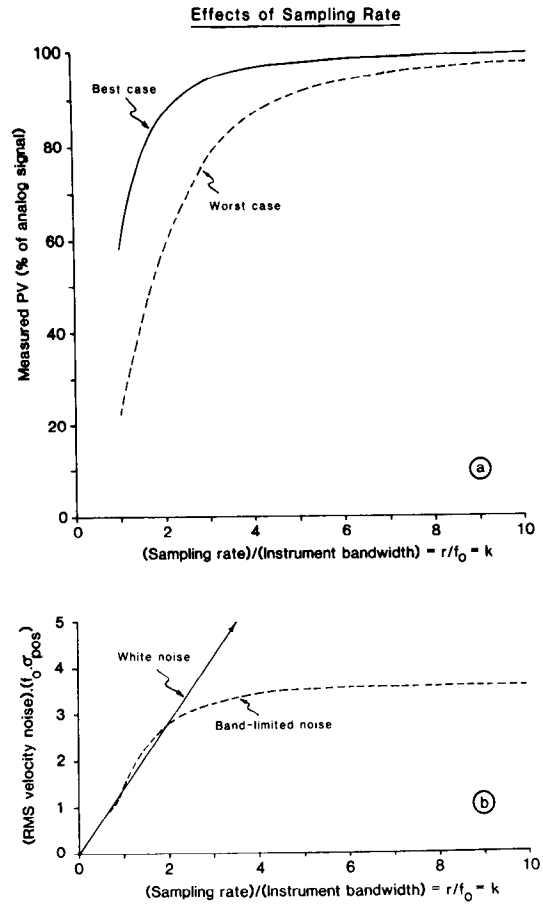

Figure 4. Effect of sampling rate on the measurement of peak velocity (PV) and on RMS velocity noise, when the eye velocity is estimated from two consecutive samples of eye position. Instrument has bandwidth of f_0. (a) Shows best and worst cases for PV as a percentage of $2f_0$—the true analog PV at the output for a unit step input. Best case occurs when true PV is midway between samples, and worst case occurs when true PV is at a sampling point. (b) Shows RMS velocity noise for uncorrelated noise samples (solid line) and band-limited noise (dashed line). RMS velocity is shown in units of $f_0\sigma_{pos}$, where σ_{pos} is the RMS position noise.

arbitrarily small by sampling at a sufficiently high rate, but this may not always be practical and is impossible for TV-based systems. Alternatively, sampling error and quantization error in eye velocity measurements can be reduced by reconstructing the original EM; eye velocity can then be estimated from the "smooth" response, rather than from two samples of eye position. Obtaining velocity via a reconstructed position signal can be accomplished in one step by applying an appropriate digital filter (a weighted "window") directly to the position samples (Engelken, Stevens, & Wolfe, 1982). The optimal digital filter will depend on the sampling rate, the noise in the instrument's output, and the number of data points considered in the window. The reader is referred to any standard text for further details (e.g., Blackman, 1965; Hamming, 1983).

If digital filter techniques are not employed, other events, such as the beginning and end of a fast EM, cannot be determined within a sampling period. Since the start of a fast EM can occur at any time during a sample period,

its detection will have a flat probability distribution with a standard deviation of $1/\sqrt{12}r$. The detection of the end of a fast EM will suffer a similar error. The error in duration measurements could therefore have a standard deviation of $1/\sqrt{6}r$, although, since fast EMs tend to have fixed durations for a given amplitude, the errors in detecting beginning and end will probably be correlated.

Besides the possibility of inaccuracy due to coarse sampling, velocity noise will also be affected by the sampling rate. If the noise characteristics do not change in time (i.e., the noise is stationary) and the noise is additive with a mean amplitude of zero, the velocity RMS noise will be given by the standard deviation of the difference between two correlated consecutive position samples divided by the sampling interval:

$$\sigma_{\dot{v}} = \left\{2r^2[\sigma^2_{pos} - C(1/r)]\right\}^{1/2}, \quad (11)$$

where C(1/r) is the covariance of two consecutive noise samples. If the noise bandwidth is much greater than the sampling rate, then consecutive noise samples will be virtually independent with no covariance. This is illustrated by the solid line in Figure 4b. As the sampling rate increases, the RMS velocity noise will increase linearly with a slope of $\sqrt{2}$. However, if the noise source is early in the system and is subjected to the instrument's filtering profile, then the noise bandwidth will be lower than the sampling rate, in which case there will be covariance between consecutive samples and the RMS velocity noise will be less. For example, consider white noise with a spectral density given by $N_0/2$, subject to a low-pass rectangular filtering profile with cutoff frequency f_0. By deriving the covariance of two consecutive samples from the inverse Fourier transform of this noise spectrum, the RMS velocity noise can be shown to be:

$$\sigma_{\dot{v}} = \left\{2r^2\sigma^2_{pos}[1 - \sin(2\pi f_0/r)/(2\pi f_0/r)]\right\}^{1/2}. \quad (12)$$

The RMS velocity noise with sampling at k times the cutoff frequency is shown by the dotted line in Figure 4b. As the sampling rate increases, the RMS noise increases, until a maximum is reached. This maximum corresponds to the analog band-limited RMS velocity noise in Equation 9, and is equal to $\sqrt{4/3}\pi f_0\sigma_{pos}$.

In short, Figure 4 shows a tradeoff: Noise can be reduced only at the expense of accuracy. If velocities are estimated from consecutive samples, a surprisingly high sampling rate is required for a reasonable accuracy; this sampling rate is considerably more than twice the Nyquist frequency. Therefore, when feasible, digital filtering techniques should be used; but this is only successful when instrument bandwidth exceeds the highest frequency component in the velocity signal. Of course, digital filtering will not reduce band-limited noise.

When digital filtering techniques are not used (as with systems whose bandwidths are inherently too low) and velocities are estimated from consecutive samples, additional problems arise. For example, estimates of PV will be especially distorted by noise. Noise can subtract or add to the true velocity in any interval; however, in most cases only the interval to which noise has added will be picked as the peak. This is a nonlinear effect, since for slow EMs a spuriously large PV will usually be found. On the other hand, sampling will produce an underestimation of PV because, on the average, the true peak will occur within an interval and be missed; this underestimation is more pronounced for faster EMs.

Conclusions

Bandwidth. There are two conflicting bandwidth requirements for the recording of fast EMs: (1) The recording instrument should have a flat frequency response up to the maximum frequency component in the fast EM. For correctly measuring eye velocity, this component is about 50 Hz for human adults, although nonhuman fast EMs may have significantly different power spectra. (2) Bandwidth should be kept as low as possible, since noise, especially on the velocity signal, increases with bandwidth.

Sampling. Sampling can have two distinct effects: (1) The sampling rate and sampling function can reduce the effective bandwidth; this is unavoidable with systems using standard TV video rates. (2) Sampling also causes error in the temporal localization of events, such as the beginning and end of a saccade or the occurrence of PV. Sampling problems can generally be avoided by sampling at as high a rate as feasible and employing digital filtering techniques to evaluate the EM parameters of interest.

EVALUATING A SPECIFIC VIDEO-BASED SYSTEM

To understand the dynamic properties of a specific recording system, it is necessary to know the system's filtering profile (or transfer function), H(f). The only certain method for finding H(f) is to present the instrument with several known inputs and to measure the corresponding outputs. Our instrument was an infrared corneal-reflection eye tracker based on a TV camera (Applied Science Laboratories Model 1994 Eye View Monitor; Hainline, 1981). This is a common type of TV system for EM recording. As the eye rotates, there is a differential motion of two images; the corneal reflection of the tracker's illuminator (first Purkinje image) and the pupil. The instrument analyzes this differential motion to estimate the direction of the optic axis of the subject's eye.

This instrument produces an estimate of eye position at the end of each interlaced TV field (60 Hz), and can average consecutive estimates. Averaging has the desired effect of reducing noise and increasing resolution, but has the drawback of reducing bandwidth (averaging is a simple low-pass digital filter). This additional reduction in bandwidth is illustrated by Curve c in Figure 3.

An "artificial eye" that emulated optically the first Purkinje and pupil images was used to provide known inputs to the eye tracker. It was rotated about a point equivalent to the center of rotation of an eye. By oscillating the ar-

tificial eye sinusoidally with a known amplitude at different angular frequencies, the transfer function H(f) was measured. This is shown in Figure 3 for both horizontal (Curve e) and vertical (Curve d) axes. As can be seen, the bandwidth is lower than would be predicted by sampling at TV rates even with a broad sampling function and averaging consecutive fields (Curve c). Investigation of this deficit indicated that the persistence of the response of the TV camera's vidicon tube extended beyond one sampling period. This persistence lengthens the instrument's time constant and reduces the bandwidth still further.

As shown earlier, twice the area under a transfer function is equal to the PV of the response of the instrument to a step input (Equation 7). The areas under the transfer functions in Figure 3 (Curves d and e) were about 15 and 20 Hz. Thus, for horizontal EMs, the greatest PV that can be registered for a 10° input is about 300°/sec. However, with this instrument we have recorded adult saccades with PVs in excess of this theoretical limit. This discrepancy suggests that the sinusoidal method of obtaining the transfer function did not truly describe the instrument. The difference in horizontal and vertical transfer functions suggests that this instrument is anisotropic in its response.

Anisotropy

An alternative procedure for describing a system is to present it with step inputs in various directions. The artificial eye could not provide a perfect step but was capable of a PV of about 1,000°/sec for a 10° excursion—much faster than a human EM of the same amplitude. It was found that rightward (in the direction of the TV raster) inputs produced outputs with PVs different from those produced by leftward inputs. The amount of this anisotropy was found to depend on the precise settings of the electronics in the TV image analyzer. This is because our particular model of instrument estimates eye position based on only the left half of the pupil and the first Purkinje images. Any persistence in the system has a differential effect depending on whether the brighter first Purkinje image is moving away from or toward the left half of the pupil image, giving rise to erroneous PVs. The vertical/horizontal anisotropy was also found to be caused by TV persistence.

Peak Velocity Calibration

Once the transfer function(s) is found, it becomes possible to "work backward" from an output to find the true input. This deconvolution process is probably worthwhile for only "clean" systems with bandwidth sufficient to embrace the input spectrum. A more tedious, but simpler, approach, more suited for noisy data and instruments with low bandwidths, is to simulate mechanically a range of inputs and record output values for specific parameters, and thus provide a set of lookup calibration curves for these parameters. Since we were interested primarily in PV, single ramps of various slopes and magnitudes were presented to the system. Although actual fast EMs do not have ramp profiles, these inputs were considered to be close enough with respect to PV and were easy to generate. The results

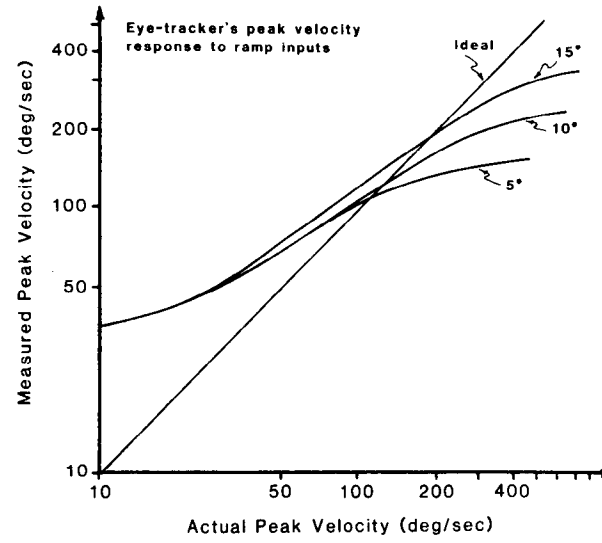

Figure 5. Peak velocity measured on the authors' instrument for ramp inputs of various slopes (abscissa) made by a mechanical "artificial eye" (see text); parametric in amplitude.

for leftward ramps are shown in Figure 5. Similar sets of curves exist for other directions. Here, the PV, as measured on the output (ordinate), is plotted against the actual ramp velocity of the input (abcissa) for three amplitudes. For example, most of our adult subjects produced 10° saccades with an apparent PV of about 200°/sec. Figure 5 indicates that the true PV was closer to 350°/sec.

Noise Measurement

By maintaining the artificial eye in a stationary position, the static RMS noise of the system was estimated. The instrument output was monitored with the artificial eye pointing in various horizontal and vertical directions. The RMS noise was found to be about 3/8° and to be independent of direction. This is in good agreement with the manufacturer's claim of 1/2° accuracy. No correlation was found between vertical and horizontal noise components. From Equation 11, a system with a 15-Hz bandwidth and a sampling rate of 60 Hz should give a RMS velocity noise of about 20°/sec. If the noise, however, originates later in the system, so that there is little covariance between noise samples, then a RMS velocity of about 30°/sec would be expected. The actual RMS velocity noise was measured to be about 22°/sec. This indicates that most of the noise originates in or before the detector and only a little noise is introduced later. This deduction was confirmed by finding the square root of the noise power spectrum and comparing its envelope to the transfer functions in Figure 3 (Curves d and e).

Discussion

As a practical demonstration of compensating for the dynamic response of our instrument, consider Figure 6 (left-hand ordinate). Here, PV is plotted against amplitude for a series of saccades from an adult human subject (a static calibration had been performed for this subject; see

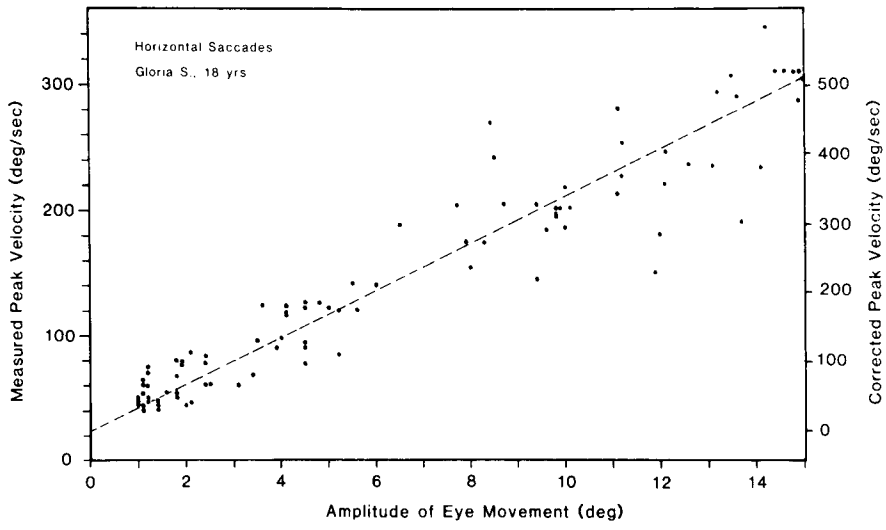

Figure 6. Left-hand ordinate—relationship between peak velocity of typical adult saccades and amplitude of saccades, as measured on the authors' instrument. Note the low slope and the nonzero intercept. Right-hand ordinate—relationship after calibration.

Harris et al., 1981). There are three main artifactual features. First, the variability in measured PV increases as PV increases. At least in part, this must be due to sampling error and cannot be reduced without incorporating signal reconstruction techniques (see "Sampling," above). Second, the slope of the PV versus amplitude relationship is much lower than that normally reported (see "Bandwidth," above). This is due to the low bandwidth of the system, as shown by Curve e in Figure 3, and can be corrected by the calibration curve in Figure 5. Third, the nonzero intercept in Figure 6 is due to velocity noise (see "Noise," above) and is also corrected by the calibration curve in Figure 5. The right-hand ordinate of Figure 6 shows the corrected PV for this subject. Thus, although this TV-based instrument falls short of the ideal in terms of dynamic response, it can, nevertheless, be used to measure fast EMs.

As stated earlier, each system must be evaluated with respect to its application. The authors' experience has been that design specifications and manufacturers' claims are no substitute for an empirical evaluation of the overall system—from the eye via the computer to the final measured EM parameter.

REFERENCES

ASLIN, R. N., & SALAPATEK, P. (1975). Saccadic localization of visual targets by the very young infant. *Perception & Psychophysics*, **17**, 293-302.

BLACKMAN, R. B. (1965). *Data smoothing and processing*. Reading, MA: Addison-Wesley.

BRONSON, G. (1982). *The scanning patterns of human infants: Implications for visual learning*. Norwood, NJ: Ablex.

BULLINGER, A., & KAUFMANN, J. L. (1977). Technique d'enregistrement et d'analyse des mouvements oculaires. *Perception*, **6**, 345-353.

CARMODY, D. P., KUNDEL, H. L., & NODINE, C. F. (1980). Performance of a computer system for recording eye fixations using limbus reflection. *Behavior Research Methods & Instrumentation*, **12**, 63-66.

CHAMPENEY, D. C. (1973). *Fourier transforms and their physical applications*. London: Academic Press.

COLLINS, C. C. (1974). The human oculomotor control system. In G. Lennerstrand & P. Bach-y-Rita (Eds.), *Basic mechanisms of ocular motility and their clinical implications* (pp. 145-182). Oxford: Pergamon Press.

ENGELKEN, E. J., STEVENS, K. W., & WOLFE, J. W. (1982). Application of digital filters in the processing of eye movement data. *Behavior Research Methods & Instrumentation*, **14**, 314-319.

HAINLINE, L. (1981). An automated eye movement recording system for use with human infants. *Behavior Research Methods & Instrumentation*, **13**, 20-24.

HAITH, M. M. (1980). *Rules that babies look by: The organization of newborn visual activity*. Hillsdale, NJ: Erlbaum.

HAMANN, K. (1979). Verlangsamte Sakkaden bei verschiedenen neurologischen Erkrankungen. *Ophthalmologica, Basel*, **178**, 357-364.

HAMMING, R. W. (1983). *Digital filters* (2nd ed.). Englewood Cliffs, NJ: Prentice Hall.

HARRIS, C. M., HAINLINE, L., & ABRAMOV, I. (1981). A method for calibrating an eye-monitoring system for use with infants. *Behavior Research Methods & Instrumentation*, **13**, 11-17.

HOWARD, I. P. (1982). *Human visual orientation*. New York: Wiley.

KLIEGL, R., & OLSON, R. K. (1981). Reduction and calibration of eye monitor data. *Behavior Research Methods & Instrumentation*, **13**, 107-111.

LEVY-SCHOEN, A., & O'REGAN, K. (1979). The control of eye movements in reading. In P. A. Kolers, M. E. Wrolstad, & H. Bouma (Eds.), *Processing of visible language I* (pp. 7-36). New York: Plenum.

MCCONKIE, G. W. (1981). Evaluating and reporting data quality in eye movement research. *Behavior Research Methods & Instrumentation*, **13**, 97-106.

MENDELSON, M. J., HAITH, M. M., & GOLDMAN-RAKIC, P. S. (1981). Monitoring visual activity in infant rhesus monkeys: Method and calibration. *Behavior Research Methods & Instrumentation*, **13**, 709-712.

PIERCE, J. R., & POSNER, E. C. (1980). *Introduction to communication science and systems*. New York: Plenum.

ROBINSON, D. A. (1981). The use of control systems analysis in the neurophysiology of eye movements. *Annual Review of Neuroscience*, **4**, 463-503.

YOUNG, L. R., & SHEENA, D. (1975). Survey of eye movement recording methods. *Behavior Research Methods & Instrumentation*, **1**, 397-429.

ZEE, D. S., OPTICAN, L. M., COOK, J. D., ROBINSON, D. A., & ENGEL,

W. K. (1976). Slow saccades in spinocerebellar degeneration. *Archives of Neurology*, **33**, 243-251.

ZEE, D. S., & ROBINSON, D. A. (1979). A hypothetical explanation of saccadic oscillations. *Annals of Neurology*, **5**, 405-414.

ZUBER, B. L., SEMMLOW, J. L., & STARK, L. (1968). Frequency characteristics of the saccadic eye movement. *Biophysical Journal*, **8**, 1288-1298.

NOTE

1. A more comprehensive derivation of the formulae presented here can be supplied upon request.

(Manuscript received February 7, 1984;
revision accepted for publication July 11, 1984.)